Microfluidics for *in vivo* imaging of neuronal and behavioral activity in *Caenorhabditis elegans*

Nikos Chronis[1,2], Manuel Zimmer[1] & Cornelia I Bargmann[1]

The nematode *C. elegans* is an excellent model organism for studying behavior at the neuronal level. Because of the organism's small size, it is challenging to deliver stimuli to *C. elegans* and monitor neuronal activity in a controlled environment. To address this problem, we developed two microfluidic chips, the 'behavior' chip and the 'olfactory' chip for imaging of neuronal and behavioral responses in *C. elegans*. We used the behavior chip to correlate the activity of AVA command interneurons with the worm locomotion pattern. We used the olfactory chip to record responses from ASH sensory neurons exposed to high-osmotic-strength stimulus. Observation of neuronal responses in these devices revealed previously unknown properties of AVA and ASH neurons. The use of these chips can be extended to correlate the activity of sensory neurons, interneurons and motor neurons with the worm's behavior.

How neural circuits process information to generate behavior is a fundamental question in neuroscience. To address this question, one should observe an animal in a well-controlled environment, in which a specific behavior can be generated and corresponding neuronal activity monitored. Ideally such an environment should not disturb normal neuronal function and should be able to reveal the specific neuronal circuit under study.

C. elegans, with its optically accessible, stereotyped and compact nervous system, has drawn great scientific attention because of its diverse repertoire of behavioral outputs and its genetic conservation with vertebrates. Initial efforts to measure activity in the *C. elegans* nervous system relied on electrophysiological recordings from single neurons in dissected worms[1]. The recent development of genetically encoded fluorescent calcium indicators[2] has spawned an increasing interest in optical imaging approaches that permit the tracking of calcium transients in individual neurons *in vivo* in intact worms[3].

Although transgenic worms that express neuron-specific indicators can now routinely be generated, the present methods for confining and stimulating the worm during imaging are not ideal. The typical experimental setup involves application of glue onto specific segments of the worm to achieve permanent immobilization on a hydrated agar pad. Fluid-filled pipettes, temperature-controlled plates and sharp electrodes have been used in the past to deliver chemical, thermal and mechanical stimuli, respectively[4,5]. Whether the organic glue is toxic to the worm and how it influences neuronal activity are difficult to determine. Moreover, the delivery of chemical stimuli to the glued worm cannot be precisely controlled or separated from mechanical stimuli associated with fluid flow. More concerns arise when the circuit controlling locomotion is under study. The glue immobilizes the worm, not allowing muscles and stretch-receptor neurons, if any, to contract and relax normally. This mechanically restricted microenvironment might affect the function of the proprioceptive sensory neurons as well as motor neurons. Most importantly, the glue setup does not permit most behaviors to be generated, visualized, quantified or correlated to neuronal activity in real time. A system with two objectives[6] has been a welcome step toward simultaneous neuronal-behavior analysis, as has been a new system for tracking thermosensory neurons (albeit at low optical resolution) in freely moving worms[7].

Recent advances in microfabrication technology permit the construction of well-controllable microenvironments with applications ranging from cell analysis to tissue engineering[8,9]. In previous studies, microfluidic delivery systems have been used to trap and stimulate single cells and embryos[10,11]. In this work we extend the applications of microfluidics to *in vivo C. elegans* imaging. We designed and engineered microfluidic devices for trapping and stimulating single worms while monitoring their behavior and neural function. We describe two 'worm chips', each one having a distinct purpose: (i) to correlate behavior and interneuron activity and (ii) to reveal stimulus-response relationships in chemosensory neurons. Using these worm chips, we show that the activity of the AVA interneurons is directly correlated to the worm's locomotion pattern and that ASH sensory neurons have a complex multiphasic response to osmotic stimuli.

RESULTS
The behavior chip
The first microfluidic device, the behavior chip (**Fig. 1a**), permitted the analysis of forward or backward worm locomotion with simultaneous recording of neuronal activity. The behavior chip consists of a worm trap, whose dimensions (1,200 µm long × 70 µm wide × 28 µm thick) were optimized for the size of young adult

worms (a young adult worm is approximately 1 mm long and 40 μm in diameter). The width of the trap gradually decreases to 40 μm at one end, an opening too small for the worm to escape. The worm trap is microfabricated using soft lithography[12]. It consists of a silicone elastomer (PDMS), which is irreversibly attached to a glass coverslip to create a tight seal. Two holes on the PDMS, one in each side of the micro-trap, are used as the inlet and outlet for loading and unloading the worm. Worms are loaded one by one in the trap and can be squeezed out of the trap by pressurizing the inlet. The microtrap restricts the worm in the vertical direction by slightly compressing it at the thickest region of its body. That region, located in the middle of the body, occupies approximately one third of the total worm body length. The head and tail of the worm are not compressed at all, as their thickness is smaller than the thickness of the trap. Traps of different dimensions can be easily fabricated if a different degree of compression is desired, but that will affect the locomotion behavior as smaller traps tend to slow down the locomotion. Compression in the vertical direction had the important feature of keeping neuronal cell bodies in a stable plane of focus, which is critical for measuring the small changes in fluorescence intensity observed in most cases with genetically encoded calcium indicators.

Trapped young adult worms could generate and propagate a sinusoidal wave along their body length with the wave amplitude defined by the width of the microfluidic trap. This body wave was often disrupted near the middle of the worm body at the region of compression. Unlike the glued environment, in which the unrestricted part of the worm swims in the fluid phase[13], the body of the worm in the microfluidic trap locally feels the reaction force from the microfluidic wall as it bends. Perhaps as a result, the body wave propagates in a sinusoidal fashion similar to wave propagation during crawling on an agar plate, a motion pattern different from the C-bends observed in swimming or glued worms.

On an agar plate, forward locomotion of the worm is the result of a posterior-traveling body wave[14]. Similarly, backward locomotion is the result of an anterior-traveling body wave. On the behavior chip, trapped worms transmitted either posterior-traveling or anterior-traveling body waves, often switching between the two.

Using the behavior chip, we imaged calcium transients in the AVA interneuron (**Fig. 1b** and **Supplementary Video 1** online) to ask how its activity correlates with the direction of the traveling body wave. AVA neurons are classified as major command interneurons that regulate backward locomotion[15]. They receive input from mechanosensory and chemosensory neurons, and elicit transient backward locomotion that is thought to represent escape
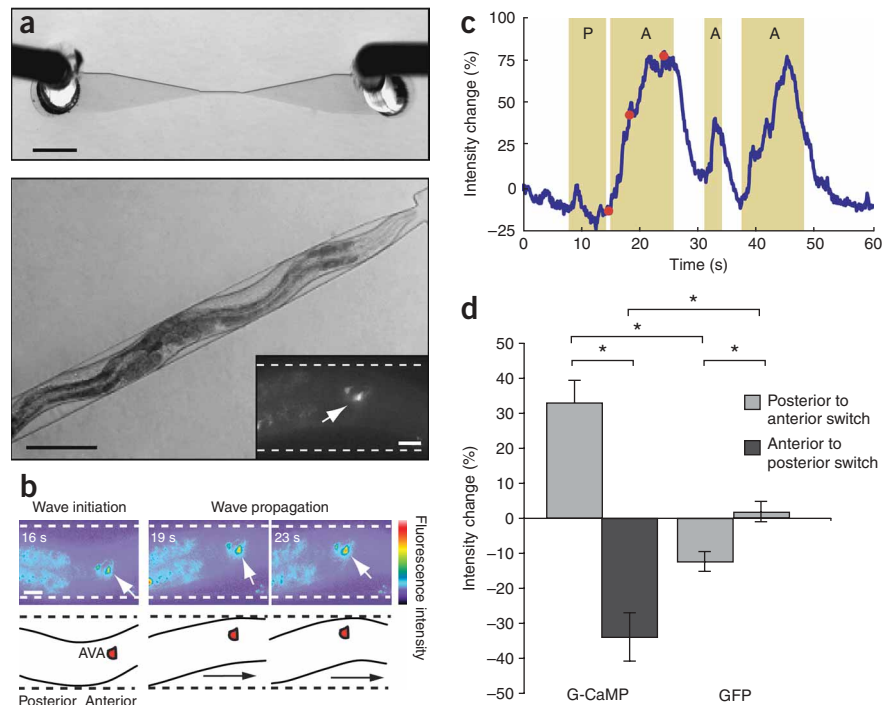
Figure 1 | The 'behavior' chip for correlating locomotion patterns with neuronal activity. (**a**) The behavior chip (top) for trapping individual worms (bottom). Inset, fluorescence image of an AVA interneuron expressing G-CaMP. Dashed lines represent microtrap walls. Scale bars, 1 mm (top), 100 μm (bottom) and 20 μm (inset). (**b**) Pseudocolor snapshots depicting change of G-CaMP intensity in AVA interneurons during worm locomotion. Pseudocolor coding indicates the scaled fluorescence intensity, ranging from no signal (black) to saturated signal (white). The schematics represent the outline of the moving worm body. Scale bar, 20 μm. (**c**) We scored anterior-traveling (A) and posterior-traveling (P) body waves and superimposed them over fluorescence traces. Unlabeled regions (regions between the shaded areas P and A) represent either a nonmoving worm or a worm with a complex locomotion pattern. The dots on the diagram correspond to the three pseudocolor snapshots at 16 s, 19 s and 23 s in **b**. (**d**) Quantification of AVA interneuron activity in G-CaMP and GFP-expressing worms. G-CaMP results represent 15 recordings from 10 worms (23 'posterior to anterior switch' events, 19 'anterior to posterior switch' events). GFP results represent 20 recordings from 15 worms (25 'posterior to anterior switch' events, 23 'anterior to posterior switch' events). $*P < 0.001$ (Student's t-test).

responses. The major synaptic output of AVA interneurons is onto motorneurons that directly innervate various sets of body-wall muscles. Laser ablation experiments have demonstrated that AVA neurons are required for normal spontaneous and evoked backward locomotion, but their precise activity has not been described.

To visualize AVA interneuron activity, we expressed the genetically encoded fluorescent calcium indicator G-CaMP[16] in the AVA neurons of wild-type worms. Despite the fact that G-CaMP signal is visualized at only a single wavelength (unlike the cameleon ratiometric sensors), we chose to use the G-CaMP sensor because of its large dynamic range[2]. As described below, the large dynamic range made it possible to quantify the small and rapid intracellular calcium changes observed during locomotion. We simultaneously recorded calcium transients in AVA interneurons and the corresponding direction of the traveling wave through the worm's body using a single 40× objective lens (**Fig. 1b,c**). The field of view of the 40× objective is approximately 180 μm or 20% of body length. When worms switched from generating a posterior-traveling body wave to generating an anterior-traveling body wave, calcium levels in AVA interneurons rose, as inferred from an average increase of 33% in G-CaMP fluorescence (**Fig. 1d**). G-CaMP fluorescence

decreased on average by 34% after the direction switched from anterior to posterior. The duration of AVA-interneuron activation varied from 2 to 45 s in 8 of 8 individual 1-min recordings from different worms switching between anterior-traveling and posterior-traveling waves. In all cases, the initiation and duration of the AVA-interneuron activation was synchronized with the initiation and duration of an anterior-traveling body wave.

Worms initiated an average of 2 anterior-traveling body waves per minute in the chip. This number is similar to the reversal frequency observed on agar plates (2.52 spontaneous reversal events per minute during the first 12 min without food; S. Chalasani, personal communication). But the duration of anterior-traveling body waves in the chip, ranging from 2 s to 45 s, was often longer than on a plate, where a typical reversal takes about 5 s. Event frequencies in the chip therefore cannot be directly compared to the probabilistic nature of events on a plate. It is possible that the physical constraints in the chip and the influence of the UV light alter the behavior pattern.

Worms generating anterior-traveling body waves appeared to move more actively in the chip than worms in other states, raising the possibility that fluorescence intensity in AVA interneurons could change artifactually because of the worm's movement. Therefore we repeated the experiments using worms that expressed conventional GFP in AVA interneurons. GFP fluorescence decreased slightly (13%) but notably in the 'posterior-to-anterior' class, reflecting the switch from forward to backward locomotion (**Fig. 1d**). This effect was opposite to the increase elicited for G-CaMP, and substantially smaller in magnitude. The decrease in the GFP fluorescence intensity may reflect a motion artifact or the intracellular pH reduction associated with calcium increase during neuronal depolarization[17]. Intracellular pH reduction in particular, induces fluorescence intensity decreases in GFP and G-CaMP signals that can be as high as 10% for a 0.1 pH unit reduction[16,18]. It is possible that this pH-dependence would cause us to underestimate real signals in the behavior chips, but it would not lead to false positive results.

The olfactory chip

We fabricated a second microfluidic device, the olfactory chip, to examine the activity of chemosensory neurons in response to chemosensory stimuli (**Fig. 2**). The 'olfactory chip' integrates a worm trap with a microfluidic chemical delivery system. The microtrap for the young adult worm is a 70 μm wide × 1,200 μm

long × 28 μm high straight microchannel that tapers to a 24-μm opening. We carefully designed the ending of the trap to match the shape and size of the worm's head. When the worm is loaded, the very end of the nose protrudes out of the trap into a flowing stream that contains the control or stimulus solution. The chemosensory cilia at the tip of the nose are always exposed to the flowing stream. If young adults are used, the body of the worm can move, as in the behavior trap; older adult worms are entirely immobilized.

The microfluidic four-flow system (**Fig. 2**) delivers the stimulus (channel 2) and the control (channel 3) solutions to the nose of the worm. Laminar flow (50–100 μl/min) ensures that minimum diffusion takes place when the two streams meet, and therefore minimal mixing occurs between the stimulus and control solutions. Under these conditions, diffusion of dissolved fluorescent dye from one stream to the other was undetectable by fluorescence imaging. A key element of the design is the presence of two additional side microchannels (channels 1 and 4) that are loaded with a fluorescein solution (20 mM in S Basal medium[19]) to visualize fluid flow. The side channels are connected to the two outputs of a three-way valve that switches the flow between them. The two dye-filled streams are used to redirect the stimulus stream toward and away from the worm's nose (**Fig. 2b**). The number of open channels (3) is constant before, during and after stimulation, minimizing pressure and flow rate changes applied to the worm.

We used the olfactory chip to monitor calcium changes in ASH sensory neurons exposed to high osmotic strength stimuli. ASH neuron is a polymodal neuron that responds to mechanical, osmotic and chemical stimuli[20]. Previous work suggested that ASH neurons expressing the genetically encoded calcium sensor
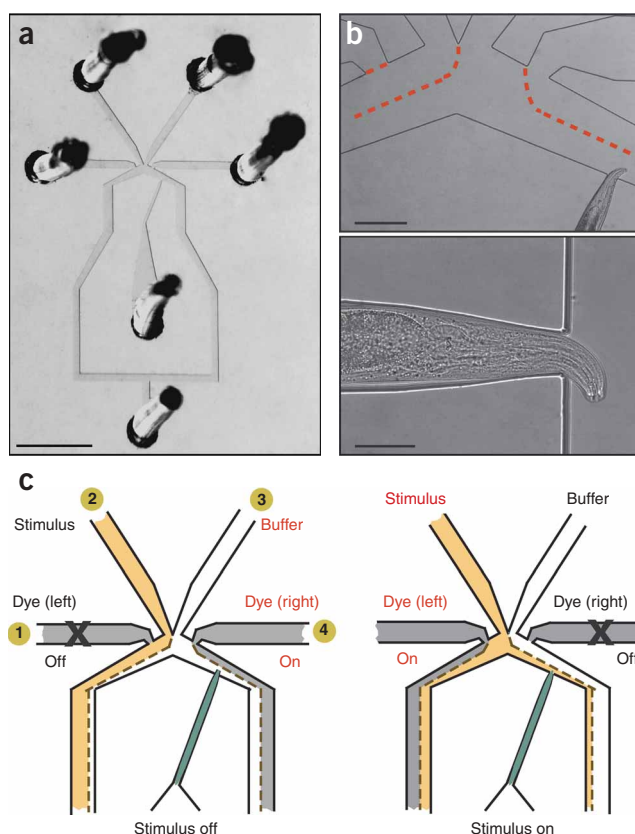
Figure 2 | The 'olfactory' chip. (**a**) The microfluidic four-flow device for delivering odor. The microfluidic chip consists of two side channels loaded with fluorescent dye (channels 1 and 4), a stimulus channel (channel 2) and a control, or buffer, channel (channel 3). Scale bar, 2 mm. (**b**) Higher-magnification photographs of the chip with a trapped worm. The dotted lines mark the interfaces between the fluids. Scale bars, 150 μm (top) and 30 μm (bottom). As shown, the nose is exposed to the buffer stream. (**c**) The stimulus and buffer streams are directed by the side flows (gray). In the 'off' state (left), the right dye channel (channel 4) is open and pushes the stimulus stream to exit from the left outlet. In the 'on' state (right), the left dye channel (channel 1) is open, and the worm is exposed to stimulus. The four-flow design minimizes pressure and flow velocity changes during stimulation. A vacuum supply (3–5 p.s.i.) is connected to the outlet of the microfluidic network to create pressure-driven flow profiles in all microfluidic channels. The inlets of the microfluidic channels are connected via polyethylene tubing to plastic syringes that are exposed to atmospheric pressure. The open ends of the syringes are 10–20 cm above the level of the chip.
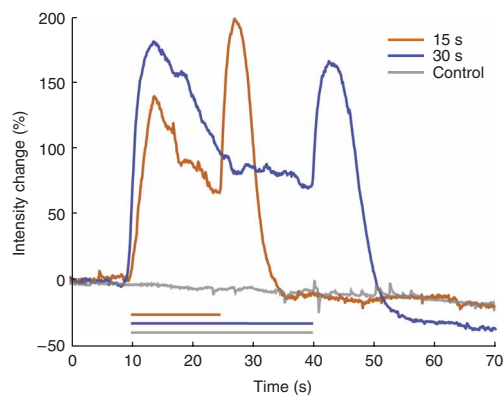
Figure 3 | Calcium transients in ASH neurons in response to a hyperosmotic stimulus. Intensity changes in the G-CaMP signal upon addition and removal of a 15-s and 30-s stimulus. In the control experiment, the stimulus and buffer channels were loaded with the same solution (S Basal medium). Each curve represents fluorescence changes obtained from individual worms. A complete set of calcium responses is available in **Supplementary Figure 1**.

cameleon respond to the presentation of osmotic repellents with transient increases in calcium levels and do not respond to stimulus withdrawal[5]. Using the olfactory chip, we found that G-CaMP–expressing ASH neurons responded to the presentation of a high-osmotic-strength stimulus (1 M glycerol diluted in S Basal medium) with a sustained calcium response, but they also responded to the removal of the high-osmolarity solution with a transient increase in calcium levels (**Fig. 3**). In all cases (10/10 worms; **Supplementary Fig. 1** online), we observed large ASH calcium transients with 100–200% changes in G-CaMP fluorescence upon removal of the osmotic stimulus. In most cases (8/10 worms), the magnitude of the transient upon stimulus removal was equivalent to or larger than the magnitude of the transient upon stimulus presentation. We observed the same biphasic pattern of ASH neuron activity when we applied a 10 mM solution of $CuCl_2$ to the worms (data not shown). Experiments using the cameleon sensor YC2.12 (ref. 21; **Supplementary Fig. 2** online) confirmed the calcium transients at the offset of hyperosmotic stimulus.

DISCUSSION

The time-resolved behavioral-imaging recordings obtained from the behavior chip supported existing evidence that AVA neurons have a central role in backward locomotion, and revealed that AVA neurons are continuously active throughout the period that the worm generates an anterior-traveling body wave. These data indicate that AVA interneurons might directly control the worm's locomotion pattern by controlling motor-neuron activity.

Although AVA neuronal depolarization is expected to precede behavior changes, we measured no apparent latency between the two processes. The time scale of our measurements (seconds) is probably too slow to visualize the first response in neurons; in addition, the cell body calcium responses that we measured with G-CaMP might trail the initial response in neuronal processes[5].

The results obtained from the olfactory chip suggest that ASH neurons have a more complex multiphasic response to osmotic stimuli than previously detected. The transient response at the end of the stimulus may have been overlooked in the past because of the

confounding effects of mechanical fluid flow in the glued worm preparation, particularly as ASH neurons are also mechanosensitive. Another reason the transient response might have been missed could be that activation of ASH neurons requires a rapid, precise removal of the high-osmolarity stimulus, which could not be easily provided in previous imaging configurations. The behavioral function of this unexpected ASH-neuron activity pattern will be the subject of future studies.

The potential use of the described technology is not limited to spontaneous movement and chemical stimulation. Microactuators or microelectrode heating elements could be included on the chip to mechanically stimulate mechanosensory neurons, or locally trigger the thermal neuronal circuit[22,23]. Designing worm traps of different widths and shapes for recording the time sequence of motor neuron activation events during locomotion should also be possible. Finally, a combined behavior-olfactory chip could enable the simultaneous monitoring of sensory, interneuronal and behavior patterns that would lead to a better understanding of how entire neural circuits function.

In conclusion, we demonstrate that microfluidic devices with precise micrometer-sized dimensions are attractive tools for the *in vivo* manipulation of small animals such as *C. elegans*. We show that it is possible to engineer microenvironments to deliver specific stimuli and record sensory neuron, interneuron and behavioral activity. We envision microfluidics as a general manipulation platform for neuronal and behavioral imaging that will contribute to the construction of a complete functional map of the *C. elegans* nervous system, providing insight into the mechanisms by which behavior is generated at the cellular level.

METHODS

Chip fabrication. We designed the chips in AutoCAD (Autodesk) and sent the design to a mask-making service (Microfabrication facility at University of California Berkeley), which provided the chrome masks. We created the master molds by spin casting at 2,800 r.p.m. (spinner model WS-400A-6NPP/LITE/IND from Laurell Technologies Corporation) and patterning a 28-μm-thick layer of SU-8-2025 photoresist (MicroChem) on bare silicon wafers. We then cast a polydimethylsiloxane (PDMS) prepolymer mixture (Sylgard 184, Dow Corning; 10:1) over the molds and cured it on a hot plate for 2 h at 70 °C. We did not find it necessary to deposit any releasing agent to the SU-8 mold before spin-casting the PDMS. After curing, we peeled off the PDMS replica from the molds, treated it with air plasma (30 W for 30 s) to activate the PDMS surface and manually attached it to the top of a glass coverslip (#1.5) to seal the chip. We created fluidic inlets and outlets in the PDMS using a sharpened, 19-gauge stainless steel needle (0.031 inch inner diameter, 0.042 inch outer diameter; Kahnetics) before bonding. We finally attached hollow steel pins (0.016 inch inner diameter, 0.025 inch outer diameter; Kahnetics) to the inlet and outlet of the chips to facilitate chip-to-tube interface.

Worm loading and calcium imaging. We performed all imaging experiments using young adult worms. To load a worm into the chip, we first placed a single worm on a food-free nematode growth medium (NGM) plate and pipetted a drop of S Basal medium[19] on the worm to make it lose contact with the agar plate. Second, we sucked the floating worm into an S Basal

medium–filled polyethylene tube (0.023 inch inner diameter, 0.038 inch outer diameter; BD Intramedic) that was maintained manually under slight vacuum with a 3 ml, plastic syringe. Third, we attached the end of the polyethylene tube to the inlet pin of the chip and injected the worm into the entrance of the chip by increasing the pressure via the manual syringe. Last, we pushed the worm into the trap by manually controlling the pressure of the microfluidic chip. At the end of each recording, we flushed the worm out of the trap by pressurizing the trap channel via the syringe and loaded a new worm in a similar fashion. In both the behavior chip and the olfactory chip, we used S Basal medium as a buffer solution. We performed all imaging experiments on a Zeiss Axioskop upright microscope equipped with a 40× oil immersion objective. Before recording from ASH neurons, we exposed the worms to fluorescent light for 1–2 min (calcium transients in ASH neurons are elicited by exposure to fluorescent light, and they can be eliminated by pre-exposure[5]). We captured time stacks of fluorescence images by real-time streaming using a CoolSnap HQ Photometrics camera with an exposure time of 80–100 ms in each frame. We performed image analysis in Metamorph software (Molecular Devices). We wrote a script in Metamorph to obtain the total background-subtracted fluorescence intensity of the cell area in each frame. We calculated the percent change of the fluorescence intensity relative to the average intensity of the first 4 s from each recording. For quantifications presented in **Figure 1d**, we calculated the difference between the average values of adjacent periods of anterior and posterior traveling body waves. We performed the ratiometric imaging in ASH neurons expressing cameleon (YC2.12) as previously described[5].

Molecular biology and generation of transgenic worms. We used the transgenic strains CX6632 (ref. 24) and CX6558 (ref. 5) to record G-CaMP and cameleon fluorescence from ASH neurons. We used an expression construct (*pMZ26*) encoding G-CaMP cDNA under the control of the *nmr-1* promoter to generate the transgenic strain CX7343 using standard procedures[25]. We performed control experiments in AVA interneurons using the strain VM484, which expresses GFP under the control of the *nmr-1* promoter[26]. In each experiment, AVA interneurons were identified as the most anterior-lateral cells expressing G-CaMP in CX7343 worms or GFP in VM484 worms.

Note: Supplementary information is available on the Nature Methods website.

AUTHOR CONTRIBUTIONS
N.C. designed the microfluidic chips, conducted the experiments, interpreted the data and wrote the paper; M.Z. designed and conducted the experiments, interpreted the data and wrote the paper; C.I.B. interpreted the data and wrote the paper.

1. Lockery, S.R. & Goodman, M.B. Tight-seal whole-cell patch clamping of *Caenorhabditis elegans* neurons. *Methods Enzymol.* **293**, 201–217 (1998).
2. Pologruto, T.A., Yasuda, R. & Svoboda, K. Monitoring neural activity and [Ca^{2+}] with genetically encoded Ca^{2+} indicators. *J. Neurosci.* **24**, 9572–9579 (2004).
3. Kerr, R. *et al.* Optical imaging of calcium transients in neurons and pharyngeal muscle of *C. elegans*. *Neuron* **26**, 583–594 (2000).
4. Suzuki, H. *et al. In vivo* imaging of *C. elegans* mechanosensory neurons demonstrates a specific role for the MEC-4 channel in the process of gentle touch sensation. *Neuron* **39**, 1005–1017 (2003).
5. Hilliard, M.A. *et al. In vivo* imaging of *C. elegans* ASH neurons: cellular response and adaptation to chemical repellents. *EMBO J.* **24**, 63–72 (2005).
6. Faumont, S. & Lockery, S.R. The awake behaving worm: simultaneous imaging of neuronal activity and behavior in intact animals at millimeter scale. *J. Neurophysiol.* **95**, 1976–1981 (2006).
7. Clark, D.A., Gabel, C.V., Gabel, H. & Samuel, A.D.T. Temporal activity patterns in thermosensory neurons of freely moving *C. elegans* encode spatial thermal gradients. *J. Neurosci.* **27**, 6083–6090 (2007).
8. Thorsen, T., Maerkl, S.J. & Quake, S.R. Microfluidic large-scale integration. *Science* **298**, 580–584 (2002).
9. Griffith, L.G. & Naughton, G. Tissue engineering—current challenges and expanding opportunities. *Science* **295**, 1009–1014 (2002).
10. Wheeler, A.R. *et al.* Microfluidic device for single-cell analysis. *Anal. Chem.* **75**, 3581–3586 (2003).
11. Lucchetta, E.M., Lee, J.H., Fu, L.A., Patel, N.H. & Ismagilov, R.F. Dynamics of *Drosophila* embryonic patterning network perturbed in space and time using microfluidics. *Nature* **434**, 1134–1138 (2005).
12. Younan, X. & Whitesides, G. Soft lithography. *Annu. Rev. Materials Sci.* **28**, 153–184 (1998).
13. Croll, A. Components and patterns in the behavior of the nematode *Caenorhabditis elegans*. *J. Zool.* **176**, 159–176 (1975).
14. Gray, J. & Lissmann, H.W. The locomotion of nematodes. *J. Exp. Biol.* **41**, 135–154 (1964).
15. Chalfie, M. *et al.* The neural circuit for touch sensitivity in *Caenorhabditis elegans*. *J. Neurosci.* **5**, 956–964 (1985).
16. Nakai, J., Ohkura, M. & Imoto, K. A high signal-to-noise Ca^{2+} probe composed of a single green fluorescent protein. *Nat. Biotechnol.* **19**, 137–141 (2001).
17. Chesler, M. & Kaila, K. Modulation of pH by neuronal activity. *Trends Neurosci.* **15**, 396–402 (1992).
18. Kneen, M., Farinas, J., Li, Y. & Verkman, A.S. Green fluorescent protein as a noninvasive intracellular pH indicator. *Biophys. J.* **74**, 1591–1599 (1998).
19. Brenner, S. The genetics of *Caenorhabditis elegans*. *Genetics* **77**, 71–94 (1974).
20. Kaplan, J.M. & Horvitz, H.R. A dual mechanosensory and chemosensory neuron in *Caenorhabditis elegans*. *Proc. Natl. Acad. Sci. USA* **90**, 2227–2231 (1993).
21. Nagai, T. *et al.* A variant of yellow fluorescent protein with fast and efficient maturation for cell-biological applications. *Nat. Biotechnol.* **20**, 87–90 (2002).
22. Jager, E.W., Smela, E. & Inganas, O. Microfabricating conjugated polymer actuators. *Science* **290**, 1540–1545 (2000).
23. Gaitan, M. & Locascio, L.E. Embedded microheating elements in polymeric micro channels for temperature control and fluid flow sensing. *J. Res. Natl. Inst. Stand. Technol.* **109**, 335–344 (2004).
24. Kahn-Kirby, A.H. *et al.* Specific polyunsaturated fatty acids drive TRPV-dependent sensory signaling *in vivo*. *Cell* **119**, 889–900 (2004).
25. Mello, C.C., Kramer, J.M., Stinchcomb, D. & Ambros, V. Efficient gene transfer in *C. elegans*: extrachromosomal maintenance and integration of transforming sequences. *EMBO J.* **10**, 3959–3970 (1991).
26. Brockie, P.J., Madsen, D.M., Zheng, Y., Mellem, J. & Maricq, A.V. Differential expression of glutamate receptor subunits in the nervous system of *Caenorhabditis elegans* and their regulation by the homeodomain protein UNC-42. *J. Neurosci.* **21**, 1510–1522 (2001).